

Scaling Up Multi-domain Semantic Segmentation with Sentence Embeddings

Wei Yin, Yifan Liu, Chunhua Shen, Baichuan Sun, Anton van den Hengel

May 1, 2024

Abstract The state-of-the-art semantic segmentation methods have achieved impressive performance on pre-defined close-set individual datasets, but their generalization to zero-shot domains and unseen categories is limited. Labeling a large-scale dataset is challenging and expensive. Training a robust semantic segmentation model on multi-domains has drawn much attention. However, inconsistent taxonomies hinder the naive merging of current publicly available annotations. To address this, we propose a simple solution to scale up the multi-domain semantic segmentation dataset with less human effort. We replace each class label with a sentence embedding, which is a vector-valued embedding of a sentence describing the class. This approach enables the merging of multiple datasets from different domains, each with varying class labels and semantics. We merged publicly available noisy and weak annotations with the most finely annotated data, over 2 million images, which enables training a model that achieves performance equal to that of state-of-the-art supervised methods on 7 benchmark datasets, despite not using any images therefrom. Instead of manually tuning a consistent label space, we utilized a vector-valued embedding of short paragraphs to describe the classes. By fine-tuning the model on standard seman-

tic segmentation datasets, we also achieve a significant improvement over the state-of-the-art supervised segmentation on NYUD-V2 [1] and PASCAL-context [2] at 60% and 65% mIoU, respectively. Our method can segment unseen labels based on the closeness of language embeddings, showing strong generalization to unseen image domains and labels. Additionally, it enables impressive performance improvements in some adaptation applications, such as depth estimation and instance segmentation.

Keywords Multi Domain, Sentence Embedding, Open World, Semantic Segmentation

1 Introduction

Semantic segmentation is a fundamental task in computer vision with numerous applications in fields such as autonomous driving, agriculture robotics, and medicine. It serves as a precursor to several downstream applications, including scene understanding and a variety of image and video editing operations. Deep learning methods have achieved remarkable success in this task through supervised training on high-quality datasets with per-pixel labels for a limited set of classes [3, 4]. However, these methods assume that all classes in testing are present during training, which is often not the case in real-world scenarios. Additionally, these models are constrained to the image domains represented in the training dataset, limiting their ability to generalize to new domains and labels. Although various approaches [5–8] have been proposed to address the open-set issues, they mainly conduct the experiment on a small dataset, which clearly limits its potential for real-world scenarios.

Wei Yin
DJI
E-mail: yvanwy@outlook.com

Chunhua Shen✉ is the corresponding author.
Zhejiang University
E-mail: chunhua@me.com

Baichuan Sun
Amazon

Yifan Liu, Anton van den Hengel
The University of Adelaide, Australia

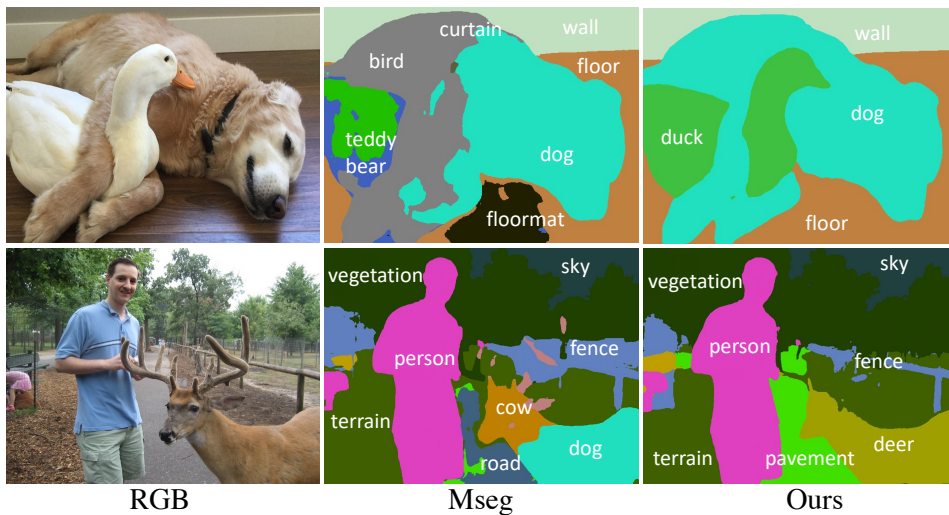


Fig. 1 Examples of segmenting zero-shot labels on web images. The labels ‘duck’ (first row) and ‘deer’ (second row) are not in the training data for Mseg [9], or the proposed method. Note that our proposed method is able to segment unseen labels successfully, however.

Training on multiple datasets from diverse domains is a natural approach to enhance a model’s robustness to variations in the statistics of data and improve generalization. However, naively merging datasets can lead to conflicting label taxonomies, as highlighted by Lambert *et al.* [9]. Lambert *et al.* proposed a laborious solution to this problem, which involves manually creating a unified label set and re-labeling the merged dataset. This is particularly challenging when datasets have semantic classes that need to be split to achieve consistency. While their approach yields well-trained models that are robust to image-domain changes, it has limitations in open-set scenarios where predefined classes are insufficient for segmentation.

Rather than attempting to manually unify a diverse set of taxonomies, and the corresponding labeled instances, here we propose a method for *automatically* merging datasets by replacing the labels therein. Specifically, for each category in each dataset, we identify a sentence describing the semantic meaning of the class. These sentences can be manually generated, but in this work are retrieved from Wikipedia. An embedding is then generated from each sentence using a language model. In this work, we use the CLIP [10] language model, but note that no image information is passed to the model, only the label sentences. Using the resulting vector-valued sentence embeddings as labels allows multiple datasets to be merged without manual intervention or inspection. The primary benefit is that it enables training on more data, from a wider variety of domains, than any single dataset can support.

By merging 9 datasets, we gain access to about 2 Million training images, which span multiple domains.

These datasets have a variety of annotation styles, however, ranging from per-pixel labels to bounding boxes. To exploit these varying annotations, we propose the heterogeneous losses that enable to leverage the noisy OpenImages [11] and weakly annotated Objects365 [12]. Our method not only significantly improves model performance and generalization ability to various domains, but also offers the advantage that *the resulting model is able to generalize to unseen labels*. This can be achieved simply by generating a new sentence describing the new class and calculating its vector-valued embedding. Applying this new vector label within the already trained model enables zero-shot segmentation of the corresponding class. Figure 1 shows some zero-shot semantic segmentation examples.

As mentioned, the sentence labels used to merge the datasets are retrieved from Wikipedia. The corresponding increase in the volume of training data available is what drives the improvement in both zero-shot and fully supervised performance to the point where both are significantly beyond the current state-of-the-art methods. Figure 3 shows the benefit of sentence-valued class labels even when the classes themselves do not overlap. The block-diagonal nature of the similarity matrix for sentence label embeddings illustrates the fact that this approach better identifies semantic similarities between classes than using an embedding of a single-word class label. Recent co-current work, Lseg [13], proposes to embed the CLIP [10] model in their system to solve the zero-shot classes segmentation problem. Owing to the robust image feature from CLIP, they can achieve impressive performance on unseen labels. In contrast, we focus on not only the unseen cate-

gories segmentation problem but also zero-shot domain generalization. Therefore, we propose to leverage sentence embeddings to solve mix-data taxonomy, which can easily scale up the training data. We train the model on a larger dataset rather than improving the techniques used in Lseg. Our method is able to exploit diverse datasets in training, which generates state-of-the-art zero-shot and fully-supervised performance as a result. The resulting model boosts the performance of related applications such as depth estimation and instance segmentation. Our main contributions are thus as follows.

- We propose a method for easily merging multiple datasets together by replacing labels with vector-valued sentence embeddings, and use the method to construct a large semantic segmentation dataset of around 2 million images.
- The semantic segmentation model trained on this combined dataset achieves state-of-the-art performance on 4 zero-shot datasets. When applied in a supervised setting (by fine-tuning), we surpass the state-of-the-art methods by over 5% on Pascal Context [2] and NYUDv2 [1]. Furthermore, our methods show the significant advantage of segmenting unseen labels.
- To solve the unbalanced annotations quality of mixed datasets, we propose a heterogeneous loss to accommodate the label noise from OpenImages [11] and leverage weakly annotated Objects365 [12].
- With the created pseudo mask labels from our model, the monocular depth estimation accuracy is improved consistently over 5 zero-shot testing datasets. Furthermore, we can surpass the fully-supervised instance segmentation method with only 25% labeled images on the COCO dataset [4].

2 Related Work

Semantic Segmentation. Semantic segmentation requires per-pixel semantic labeling, and as such represents one of the fundamental problems in computer vision. The first fully convolutional approach proposed was FCN [14], and various schemes have been developed to improve upon it. The constant increase in network capacity has driven ongoing improvements in performance on public semantic segmentation benchmarks, driven by developments such as ResNet and Transformer. Recently, stronger transformer backbones such as Segformer [15], Swin [16] have shown promises for semantic segmentation. Researchers have developed various segmentation models by, *e.g.*, investigating larger receptive fields, and exploiting contextual information.

Zero-shot Semantic Segmentation. The term zero-shot has multiple meanings, including both applying a model to a dataset that it has not been trained on [9] [17], and using a pre-trained model to identify novel classes [5] [6]. The first category focuses on solving the zero-shot domain transferring problem. Most current semantic segmentation methods [18,19] train the model on a specific dataset, thus with limited generalization ability to diverse scenes. To solve this problem, Mseg proposes a unified taxonomy to set up large-scale data for training, while wildash [17] proposes an evaluation benchmark. Furthermore, how to segment the categories that have never been seen during training is a relatively new research topic [6, 7]. Existing zero-shot categories segmentation methods can be categorized into 2 streams, *i.e.* discriminative methods [6–8] and generative methods [20–22]. Xian *et al.* [5] proposed a discriminative zero-shot semantic segmentation method, which transfers each pixel’s feature to a semantic word embedding space and obtains the class probability via the distance to the fixed semantic word embedding. Similarly, Zhao *et al.* [8] proposed a discriminative method to solve the zero-shot semantic segmentation problem using a label hierarchy. They thus incorporate hypernym/hyponym relations from WordNet [23] to help with zero-shot parsing. Hu *et al.* [6] argued that the noisy training data from seen classes challenge the zero-shot label transfer. To address this issue, they proposed an approach based on Bayesian uncertainty estimation. Baek *et al.* [7] proposed to align the visual and semantic information through a learned joint embedding space and introduce boundary-aware regression and semantic consistency losses to learn discriminative features. In contrast, the ZS3Net [20] is a typical generative method. They propose a generative model to generate per-pixel features by word embeddings and train it in a supervised manner. As the text embeddings are designed to describe the objects instead of pixels, ZS3Net’s formulation is not robust. To create diverse and context-aware features from semantic word embeddings, Gu *et al.* [21] proposed a contextual module to capture the pixel-wise contextual information in CaGNet. A variety of zero-shot methods have followed [6] [23] [20]. Existing methods are primarily either generative or discriminative. In contrast to these pixel-wise zero-shot classification methods, Ding *et al.* [22] proposes decoupling the mask segmentation and multi-class classification problems. They first implement a class-agnostic segmentation and then combine it with CLIP [10] to solve the category classification.

The approach that we propose is applicable to both versions of the zero-shot problem. We demonstrate robust performance in both settings. It is most notable,

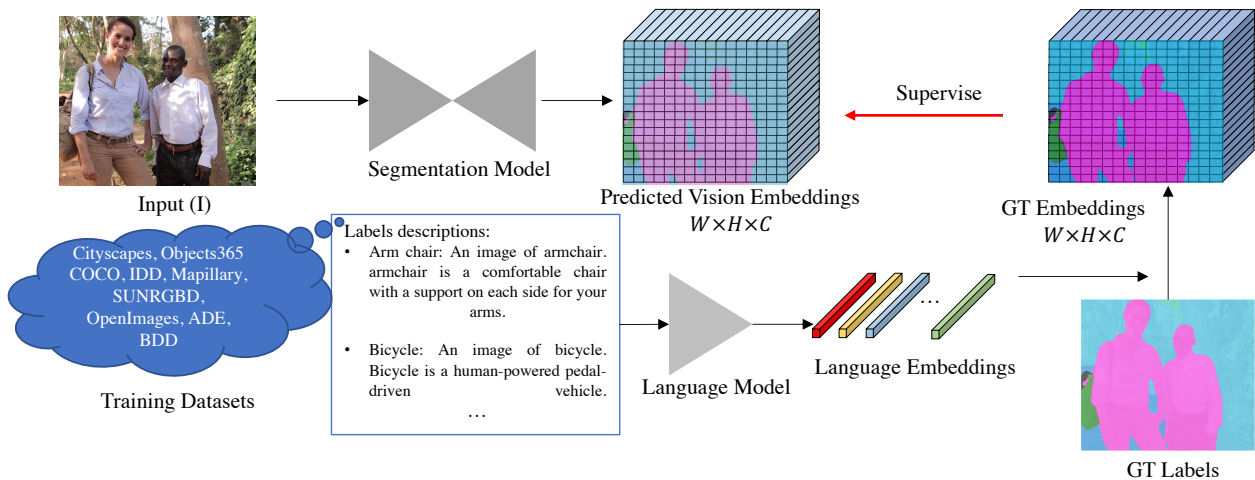


Fig. 2 Our framework. We merge multiple datasets together and encode all labels to embeddings using a language model. The semantic segmentation model is enforced to learn pixel-wise embeddings. During testing, the cosine similarity between the predicted embedding and the search embedding space is calculated. The output class is the most similar one in the label space.

however, that our method achieves a level of accuracy on each of the 7 major datasets, without training on them, that matches that of the fully-supervised approaches.

Domain-agnostic Dense Prediction. There have been a range of methods that merge segmentation datasets to improve performance and generalization, including Ros *et al.* [24] who combined six driving datasets, and Bevandic *et al.* [25] who aggregated four datasets for joint segmentation and outlier detection on WildDash [17] (a benchmark designed for cross-domain robustness evaluation). As mentioned above, Lambert *et al.* [9] proposed a method for creating a consistent taxonomy to unite datasets from multiple domains. They achieve strong generalization over multiple zero-shot datasets. Apart from semantic segmentation, the generalization to diverse scenes is also an issue for monocular depth estimation. Recent methods try to solve it by leveraging better learning objectives [26] [27] [28] [29] [30] for mixed datasets training [31] [32]. They have achieved impressive performance in zero-shot domain transfer settings.

Encoding Labels for Zero-shot Learning. Many zero-shot methods have generated semantic embeddings for class labels, and multiple methods for mapping between semantic embeddings and visual features have been devised. For example, Bucher *et al.* [20] use Word2Vec [33] to encode the labels, and is the only example that we are aware of in semantic segmentation. Recent examples that apply this approach for other purposes include Bujwid *et al.* [34] and CLIP [10]. A co-current work LSeg also uses language embeddings to supervise the class labels in semantic segmentation.

3 Proposed Method

Figure 2 shows the overview of our method. Current semantic segmentation methods feed an RGB image $I \in \mathcal{R}^{W \times H \times 3}$ to a neural network and predict per-pixel classes $p \in \mathcal{R}^{W \times H \times N}$, where N is the number of predetermined classes.

Recently, CLIP [10] shows promising robustness by leveraging natural language supervision for image classification on a large-scale dataset. Inspired by this, instead of using one-hot vectors to represent the predefined labels, we employ language models to encode semantic labels into embedding vectors. In our experiments, we use the CLIP-ViT language model to encode all labels. The encoded language embeddings are $e \in \mathcal{R}^{N \times C}$, where C is the embedding dimension. The vision embeddings from the segmentation model are $\mathcal{V} = \phi(I) \in \mathcal{R}^{W \times H \times C}$.

Creating Language Embeddings. To train a robust model, we merged 9 datasets together for training, containing 238 labels in total. Lambert *et al.* [9] manually create a unified label list and encode each label in a one-hot vector. All labels are independent to each other. In contrast, we employ a soft semantic embedding to replace the original labels, which can retain the relations among labels. Such relations are important for segmenting zero-shot labels.

Ideally, the closeness between embeddings is positively correlated to the similarity between different labels. For example, ‘Pedestrian’ should be close to ‘Rider’ but far from ‘Animals’ and other objects. Recently, several zero-shot semantic segmentation and classification methods [20] [7] [6] explore pre-trained linguistic semantic features using class names (*i.e.*, word2vec).

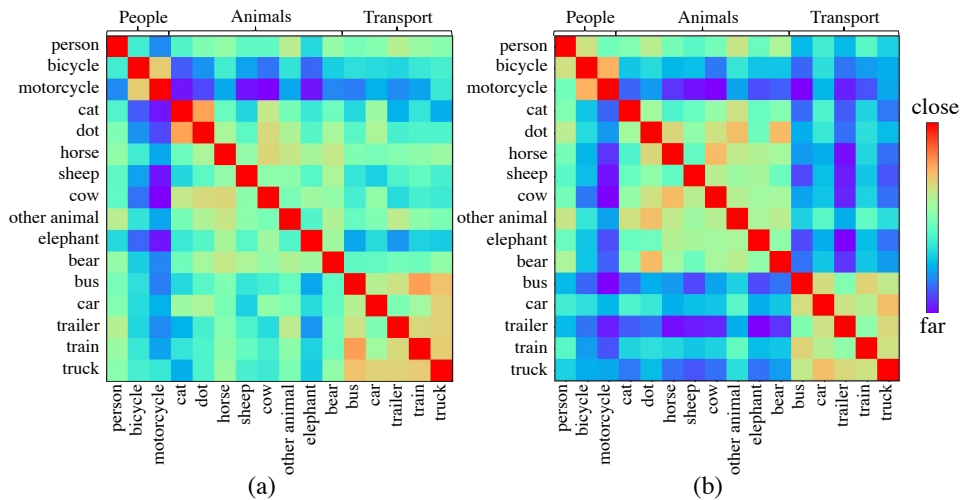


Fig. 3 A visualisation of the pairwise distances between label embeddings for (a) single word class labels and (b) sentences. The sentence embeddings better reflect the underlying semantic similarity between classes. For example, ‘Animals’ classes are close to each other but far from those in ‘People’ and ‘Transport’. Capturing and exploiting these semantic similarities in diverse datasets can improve both zero-shot, and fully supervised segmentation performance.

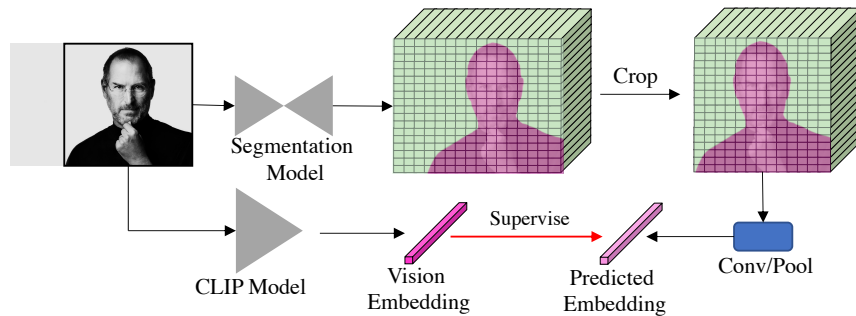


Fig. 4 Distillation pipeline for weakly-labeled data. We use the clip classification model to obtain the vision embedding for the bounding box regions. It is applied to supervise the predicted bounding box embedding.

The problem is that words are sensitive to linguistic issues and can give little discriminability of classes. Some names may partially overlap or not well reflect semantic similarity. For example, ‘counter’ can be a counting device or a long flat-topped fitment. By contrast, textual descriptions are rich in context information. We thus collect short descriptions from Wikipedia to represent each label. For example, ‘bus: An image of bus. A bus is a road vehicle designed to carry many passengers.’ Figure 3 visualizes the cosine similarity matrix of embeddings, which are created from words or sentences. The block-diagonal nature demonstrates that our sentences embeddings better represent the semantic similarities. For example, classes in ‘Animals’ are close to each other but far from those in ‘People’.

Heterogeneous Constraints for Mixed Data Training. To obtain a robust segmentation model, we merge 9 datasets for training, including 7 well-annotated datasets, a coarsely-annotated dataset (OpenImages [11]), and a weakly annotated dataset (Objects365 [12]). Owing to the unbalanced quality, we propose to employ hetero-

geneous losses to train the model. For well annotated datasets, we enforce a pixel-wise loss on all samples. The loss function is as follows.

$$z_{i,j} = \frac{e_j \cdot \mathcal{V}_i}{\|e_j\| \|\mathcal{V}_i\|}, i \in [0, M], j \in [0, N] \quad (1)$$

$$l_i = \frac{\exp(z_{i,j}/\tau)}{\sum_{j=0}^N \exp(z_{i,j}/\tau)} \quad (2)$$

$$L_{\text{HD}} = -\frac{1}{M} \sum_{i=0}^M y_i \log(l_i) \quad (3)$$

where M is the number of valid pixels, N total categories, y_i is the ground-truth labels, and τ is the learnable temperature. e is the created language embeddings of training labels, while \mathcal{V} is the predicted vision embeddings.

As a coarsely annotated dataset contains many noises, we observe that directly enforcing the above pixel-wise loss leads to worse results. Figure 5 shows some noisy annotations from the OpenImages dataset. To alleviate the effect of such noises, we propose to enforce the loss

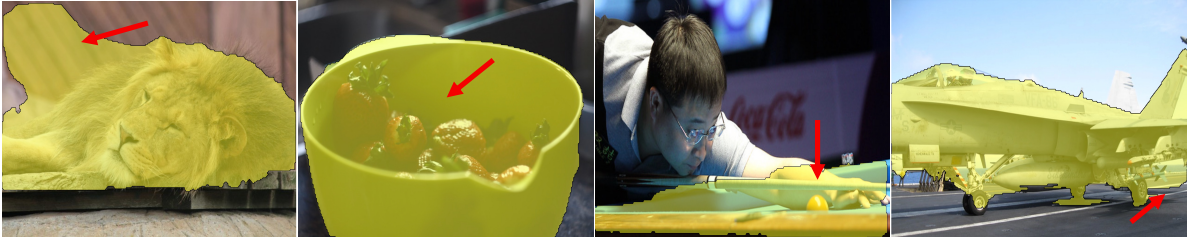


Fig. 5 Examples of noisy annotations from OpenImages (see red arrows regions). Left to right: masks for lion, bowl, billiard table, and airplane.

on some high-confident samples and ignore the noisiest parts. The loss functions are as follows:

$$w_i = \begin{cases} 0, & \log(l_i) > \mu \\ 1, & \log(l_i) \leq \mu \end{cases} \quad (4)$$

$$L_{LD} = -\frac{1}{M} \sum_{i=0}^M w_i \cdot y_i \log(l_i), \quad (5)$$

where μ is an adaptive threshold. In our experiments, we rank all samples' losses of each image and set μ to the highest 30% loss value. Each image has an adaptive threshold. With the proposed heterogeneous loss for OpenImages, we can obtain much better segments (see Figure 7).

Furthermore, we propose a distillation method to leverage the weakly annotated dataset, Objects365, which only contains bounding boxes for foreground objects. Specially, since the CLIP classification model has obtained robust knowledge of image contents, we distill such knowledge to our segmentation model on box-level annotations.

We crop and resize the bounding box from the image $I_r = (crop(I, r))$ and feed it to the CLIP classification model to obtain the vision embedding for objects, $\mathcal{V}_r^* = \mathcal{G}(I_r)$. I is the image and r is the bounding box. To retrieve the predicted bounding box embedding, we crop the corresponding region $crop(\mathcal{V}, r)$ from the segmentation embeddings and enforce a 1×1 convolution and ROI pooling on that $\mathcal{V}_r = \text{RoI}(crop(\mathcal{V}, r))$. Lastly, we apply the ℓ_1 loss to minimize their distance. The pipeline is shown in Figure 4.

$$\mathbf{v}_r^* = \frac{\mathcal{V}_r^*}{\|\mathcal{V}_r^*\|}, \mathbf{v}_r = \frac{\mathcal{V}_r}{\|\mathcal{V}_r\|} \quad (6)$$

$$L_{WD} = \frac{1}{P} \sum_r \|\mathbf{v}_r^* - \mathbf{v}_r\|_1 \quad (7)$$

where P is the number of bounding boxes. The overall loss is as follows:

$$L = L_{HD} + L_{LD} + L_{WD}, \quad (8)$$

During inference, we calculate the cosine similarity between predicted vision embeddings and created language embeddings to obtain pixel-wise labels.

Testing data for Semantic Segmentation		Testing Data for Downstream Applications	
CamVid [40]	Test set	Depth Estimation	
Pascal VOC [2]	Validation set	NYUv2	Test set
Pascal Context [41]	Validation set	KITTI	Test set
KITTI [42]	Test set	DIODE [43]	Test set
Wilddash1 [17]	Validation set	ScanNet [44]	Validation set
Wilddash2 [17]	Test set	Sintel [45]	Validation set
Youtube VIS [46]	Sampled data	Instance Segmentation	
NYUv2 [1]	Test set	COCO [4]	Validation set

Table 1 Datasets employed in our experiments for evaluation.

4 Experiments

4.1 Datasets and Implementation Details

In our experiments, we merged multiple datasets together for training and tested on 13 zero-shot datasets to evaluate the robustness of our method.

Training Data. We firstly merged 7 high-quality annotated semantic segmentation datasets (HD), including ADE20K [35], Mapillary [36], COCO Panoptic [4], India Driving Dataset (IDD) [37], BDD100K (BDD) [38], Cityscapes [3], and SUNRGBD [39]. Apart from that, we sample some data from the instance segmentation dataset OpenImagesV6 [11] (OI) and weakly annotated dataset Objects365 [12] (OB) for training. Note that OpenImagesV6 only contains noisy foreground objects masks, while Objects365 provides objects bounding box annotations. These high-quality datasets (HD) have over 200K images. OpenImagesV6 has around 700K images, while Objects365 has over 1M images.

Testing Data for Semantic Segmentation. To evaluate the robustness and effectiveness of our semantic segmentation method, we test on 8 zero-shot datasets, including CamVid [40], KITTI, Pascal VOC, Pascal Context, ScanNet [44], WildDash1 [17], WildDash2 [17], YoutubeVIS [46]. Furthermore, we fine-tune our well-trained model on NYUv2 [1] and Pascal Context to show our method can provide strong performance.

Testing Data for Downstream Applications. We create pseudo-semantic labels on zero-shot datasets to boost downstream applications, including instance segmentation and monocular depth estimation. We create

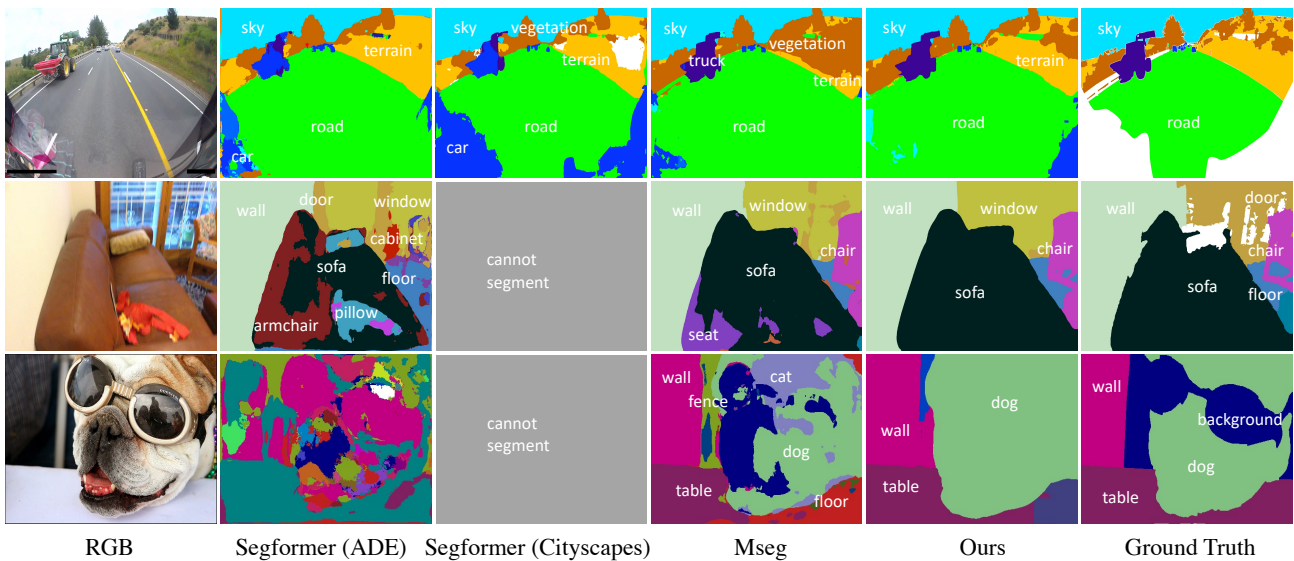


Fig. 6 Qualitative comparison on some zero-shot datasets (Pascal Context, ScanNet, and Wilddash1). Comparing with current methods, our method can retrieve better results.

pseudo instance masks on Objects365 to help instance segmentation on COCO [4]. For depth estimation, following LeReS [32], we create pseudo semantic masks on 9 RGBD datasets, of which 4 datasets are employed for training and others are for zero-shot depth evaluation, including NYUDv2, KITTI, DIODE [43], ScanNet, and Sintel [45]. More details are shown in Table 1.

Evaluation Metrics. We employ the mean intersection over union (mIoU) to evaluate semantic segmentation and AP [4] for the instance segmentation. Following [31] [32], we take absolute relative error (AbsRel) and percentage of pixels satisfying:

$$\delta_\tau = \max\left(\frac{d_{pred}}{d_{gt}}, \frac{d_{gt}}{d_{pred}}\right) < \tau$$

for evaluation. d_{gt} and d_{pred} are ground-truth and predicted depth respectively.

Multi-scale Evaluation for Semantic Segmentation. When evaluating the semantic segmentation performance, we employ multi-scale testing. We resize the testing images into multiple scales to feed into the model, i.e. with scales of 0.5 to 1.75 with 0.25 increments. Then we average the scores as the final prediction.

Implementation Details. We use two network architectures in our experiments, HRNet-W48 [52] and Segformer [15]. When training HRNet, we use SGD with momentum and polynomial learning rate decay, starting with a learning rate of 0.01. For the Segformer network, we use AdamW with polynomial learning rate decay and an initial learning rate 0.00006. To train a robust model on multiple datasets, following [53], we balance all datasets in a mini-batch to ensure each dataset

accounts for an almost equal ratio. During training, images from all datasets are resized such that their shorter edge is resized to 1080. We randomly crop the image by 713×713 for HRNet and by 640×640 for Segformer. Other data augmentation methods are also applied, including random flip, color transformations, image blur, and image corruption. In the inference, we resize the image with the short edge to one of three resolutions (480/720/1080). When comparing with existing methods, multi-scale (ms) or single-scale (ss) testing is employed.

4.2 Semantic Segmentation Evaluation

To demonstrate the robustness and effectiveness of our methods, we conduct evaluation on 15 datasets.

Robustness Evaluation. To show the robustness of our method, we firstly compare with existing state-of-the-art methods on 6 zero-shot datasets (unseen to our method during training). Note that current methods have been trained on testing datasets. Results are shown in Table 2. Our method can achieve state-of-the-art performance on CamViD, ScanNet, and WildDash1. Besides, we list the performance of HRNet [52] trained on an individual training dataset. We can see that our method, trained on mixed datasets, shows much better robustness than them. Furthermore, Mseg [9] laboriously merged 7 well-annotated datasets and craftily designed a unified taxonomy for labels mapping. It shows strong generalization over these zero-shot testing datasets. By contrast, our methods, using sentences to automatically establish the label’s closeness, achieves much bet-

Methods	CamVid	KITTI	VOC	Pascal Context	ScanNet	WildDash1	H-Mean
State-of-the-art methods on corresponding benchmarks							
Zhu <i>et al.</i> [47]	81.7	-	-	-	-	-	-
Chroma UDA [48]	-	60.4	-	-	-	-	-
AutoDeepLab [49]	-	-	82.0	-	-	-	-
DeepLabV3+ [50]	-	-	-	54.5	-	-	-
Valada <i>et al.</i> [51]	-	-	-	-	52.9	-	-
HRNet trained on a single dataset, zero-shot testing							
HRNet [52] (COCO)	56.6	48.2	73.7	43.1	33.9	38.9	46.0
HRNet (ADE)	53.5	44.3	34.6	24.0	43.8	37.0	37.1
HRNet (Mappillary)	82.5	68.5	22.0	13.5	2.1	55.2	9.2
HRNet (IDD)	70.5	50.7	14.5	6.3	1.6	40.6	6.5
HRNet (BDD)	71.0	55.0	13.5	6.9	1.4	52.1	6.1
HRNet (Cityscapes)	65.3	58.1	12.1	6.5	1.7	30.1	6.7
HRNet (SUN)	0.1	0.7	10.2	4.3	42.2	1.4	0.3
Methods trained on mixed datasets, zero-shot testing							
MSeg [9]	82.4	62.4	70.8	45.2	48.4	64.2	59.6
Ours_HRNet	83.4	66.9	74.9	48.6	52.0	64.0	62.6
Ours_Segformer	83.7	68.9	<u>81.1</u>	<u>54.2</u>	55.3	69.7	66.9

Table 2 Quantitative comparison to existing methods on 6 zero-shot (unseen during training) datasets. Current state-of-the-art methods are trained on corresponding testing datasets, while other methods have never seen them during training. Our method achieves better performance than existing state-of-the-art methods on CamVid, ScanNet, and WildDash1, and is on par with existing methods on others. Compared with Mseg and HRNet trained on a single dataset, our methods is more robust in zero-shot testing. H-mean represents the Harmonic mean for all datasets.

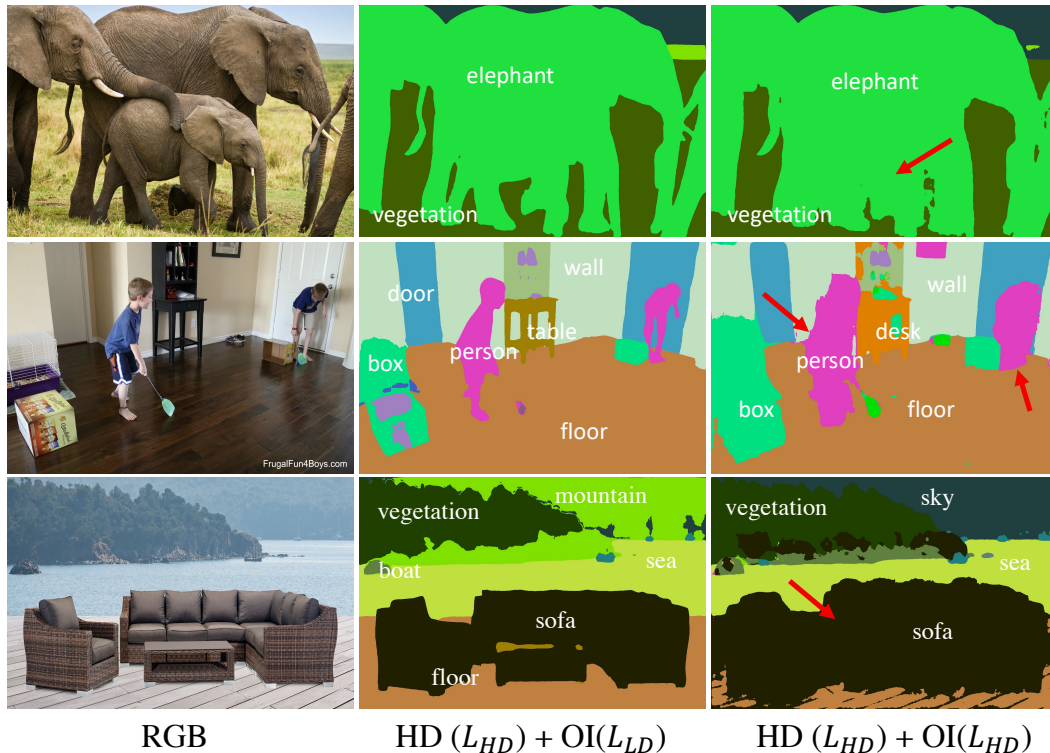


Fig. 7 Effectiveness of heterogeneous loss. We test on some google images. With the proposed heterogeneous loss, the segmented results are much more accurate. Red Arrows highlight some comparisons.

ter performance than them over all zero-shot testing data. Furthermore, we show the performance compari-

Methods	COCO	ADE	Mapillary	IDD	BDD	Cityscapes	SUN	H-Mean
Mseg	48.6	42.8	51.9	61.8	63.5	76.3	46.1	53.9
Ours_HRNet	53.3	48.4	55.3	65.0	69.0	79.2	50.5	58.4
Ours_Segformer	64.6	55.1	59.1	67.0	70.5	82.9	50.5	62.8

Table 3 Quantitative comparison of our method with Mseg on the validation set of training data. Our method achieves better performance than them over all datasets.

	mIoU
Mseg [9]	34.6
Porzi [54]	37.1
Ours	37.9

Table 4 Comparison with state-of-the-art methods on Wilddash2.

Methods	Arch.	Training Data	CamVid	KITTI	VOC	Pascal Context	ScanNet	Wildash1
Ours	HRNet-W48	HD	82.8	63.8	71.6	45.8	46.3	63.4
Ours	HRNet-W48	HD+OB	83.4	66.0	74.6	48.3	49.8	63.4
Ours	HRNet-W48	HD+OI	83.4	66.9	74.9	48.6	52.0	64.0
Ours	Segformer-B5	HD	83.6	66.5	79.9	53.0	53.0	68.2
Ours	Segformer-B5	HD+OI+OB	83.7	68.9	81.1	54.2	55.3	69.7

Table 5 Effectiveness of add weakly-annotated data and noisy data with our proposed heterogeneous losses.

Method	Lizard	Shark	Frog	Deer	duck	Mean
	mIoU (ss)					
JoEm [7]	6.3	20.3	15.9	5.1	11.5	11.8
Mseg [9]	-	-	-	-	-	17.3
Ours (Word)	13.1	11.2	11.1	4.2	22.8	12.5
Ours (Sentence)	23.6	51.6	25.8	17.8	36.1	31.0

Table 6 Comparison of zero-shot labels on the YoutubeVIS dataset. We compare with Mseg and a zero-shot semantic segmentation method, JoEm. As these labels do not exist in Mseg predetermined categories, we can only evaluate their animals mask accuracy on these labels. By contrast, JoEm and our method can segment these zero-shot labels. Our method, using the sentence description to create language embeddings, can achieve much better performance than others.

son on the validation set of training data in Table 3. Our well-trained model outperforms Mseg over all datasets.

Evaluation on Wilddash2. The Wilddash2 benchmark is intended for testing the robustness of models trained on other datasets, and does not provide a training set of its own. Our method achieves the state-of-the-art performance on it. Results are shown in Table 4.

Effectiveness of Aggregating Noisy and Weak annotations with Heterogeneous Losses. We propose the heterogeneous losses to supervise the merged datasets. When aggregating OpenImages (‘HD+OI’) supervised with our $L_{HD} + L_{LD}$, Table 5 shows the performance can be improved consistently over all zero-shot datasets. Figure 7 qualitatively compares with or without L_{LD} supervision for OpenImages (OI). We collect several web images for evaluation. We can observe that without L_{LD} loss (‘HD (L_{HD}) + OI (L_{HD})’), the predicted segments are much worse. Furthermore, when merging the Objects365 (OB) with the loss L_{WD} , the performance is improved over all zero-shot datasets.

Generalization on Unseen Labels. As we employ language embeddings to represent semantic labels, the visual similarity between labels are established by text expressions. In this experiment, we aim to observe if our resulting model can segment some zero-shot categories.

Note that all these testing labels have never existed in our training data. We sampled around 2100 images with 5 zero-shot labels from YoutubeVIS [55]. Under this setting, we mainly compare with Mseg and JoEm [7] because Mseg has strong generalization over cross domains and JoEm is the current state-of-the-art zero-shot semantic segmentation methods [7]. We use their released weight for testing. JoEm is trained on the Pascal Context to segment 6 unseen classes. In contrast, as these labels are not in Mseg predetermined categories, we can only merge all their predicted animal labels to a single mask and evaluate the merged ‘animal’ mask accuracy. We cannot retrieve any category information from its results. By contrast, ideally, our method and JoEm can segment these zero-shot labels, since we can encode descriptions of labels in language embeddings. By comparing the cosine similarity between predicted embeddings and language embeddings, the semantic label can be retrieved. We compare two encoding methods: 1) encoding label words (‘Ours (Word)’) 2) encoding short descriptions (‘Ours (Sentence)’). Results are illustrated in Table 6. Our method is more robust and can achieve better performance than JoEm and Mseg. Furthermore, we can observe that using sentences can achieve much better performance.

Finetuning on Small Datasets. In this experiment, we fine-tune our model on small datasets to show our well-trained weight can boost the performance significantly. We compare our well-trained weights, HRNet-W48 and Segformer-B5, with other weights on NYUv2 [1] and Pascal Context [41]. We fine-tune the model for 100 epochs on NYU and 50 epochs on Pascal Context. Quantitative comparisons are shown in Table 4.2. Compared with ImageNet pre-trained weight (‘*(ImageNet)’), our method surpasses them by a large margin, over 5% higher. Similarly, our method is better than Mseg and ADE20K pretrained weight (‘*(Mseg)’, ‘*(ADE20K)’).

	VOC	PC	CamVid	WildDash 1	KITTI	ScanNet
Naive Merge	17.8	19.4	56.3	55.9	61.6	45.6
Human Effort	70.8	45.2	82.4	64.2	62.4	48.4
Ours	74.9	48.6	83.4	64	66.9	52

Table 7 Comparison of data merging methods for training. All the models are trained with the same network structure of HRNet. When mixing 7 high-quality data for training, we compare with the ‘Naive Merge’ and ‘Human Effort’. ‘Naive Merge’ does not solve the label conflicts when mixing multiple datasets, while ‘Human Effort’ employs a unified taxonomy for manual mapping as stated in [9]. In contrast, we employ sentence embeddings to represent labels, which can achieve better performance on mixed data training with less human effort. Note that all testing data are unseen during training.

Compared with state-of-the-art methods, our method can achieve much better performance.

Effectiveness of Distillation. To employ large-scale weakly annotated data (Object365), we propose to use CLIP to distill our model. The experiment results are reported in Tab. 5. ‘HRNet-W48 HD’ is the baseline, which trains the model on large-scale high-quality semantic segmentation data. ‘HRNet-W48 HD+OB’ merge the segmentation data with object detection data (Object365). Although we only roughly distill the knowledge on cropped bounding box regions, the performance can still achieve noticeable improvement. We hypothesize the gains come from the large-scale Object365 data and CLIP’s strong and robust semantic knowledge.

Effectiveness of Merging Training Data with Language Embeddings. How to merge training data labels is important for mixed data training. In this ablation, we compare two different approaches to solve this problem. The baseline method is to naively merge all data labels and employ a cross-entropy loss to supervise the training, see ‘Naive Merge’ in Tab. 7. We can observe that the performance on zero-shot datasets is much worse than that of Mseg, which proposes a unified taxonomy for manually mapping labels. In contrast, we propose to employ sentence embeddings to represent labels. As the sentence embeddings can represent the underlying semantic similarities between classes, which is more applicable to solving label conflicts. Our method can achieve better performance than others.

Comparison with Lseg The co-existing approach, Lseg [13], proposes a solution to perform zero-shot semantic segmentation by incorporating CLIP feature in their pipeline. In contrast, our method employs CLIP to create soft embeddings for sentences, allowing us to address the mixed-data taxonomy and enhance the model’s ability to generalize to zero-shot domains and labels by scaling up the training data. A quantitative comparison is presented in Fig. 8, where the model is evaluated on different label sets with varying levels of granularity. While both methods demonstrate comparable

performance on coarse labels, our approach produces superior segmentation results on refined labels.

4.3 Boosting Downstream Applications

Boosting Monocular Depth Estimation. We create pseudo semantic labels on multiple zero-shot depth datasets to boost monocular depth estimation. Following LeReS [32], we train monocular depth estimation model on Taskonomy [71], DIML [72], Holopix [73], and HRWSI [64] and evaluate it on 5 zero-shot datasets. On these 9 unseen datasets, we create pseudo semantic masks and transfer them to pixel-wise language embeddings, whose dimensions are 512. During training, we employ the ResNet50 backbone. The language embeddings are feed to a 1×1 convolution to reduce the dimension from 512 to 64, which is added to the depth prediction network. Then we add the transferred embeddings to the image feature after the first 7×7 convolution. The framework is shown in Fig. 9. Results are shown in Table 9. Comparing with the baseline method ‘LeReS’, adding our created embeddings can consistently improve the performance over all datasets.

Boosting Instance Segmentation. Instance segmentation is another important fundamental problem. To demonstrate that our method can boost its performance, we create pseudo instance masks on sampled Objects365. The created pseudo labels have 7000K instance masks and 73 categories. We firstly train CondInst [68] on pseudo labels and then finetune it on COCO [4]. Comparisons are illustrated in Table 10. With the ResNet-50 backbone, our method (‘Ours(CondInst), 25%COCO’), using only 25% COCO data, can achieve comparable performance with the baseline method ‘CondInst’, and can surpass other state-of-the-art methods with 50% COCO data. When finetuned on the whole COCO, our method is (‘Ours(CondInst), COCO’) around 4% AP higher than the baseline (‘CondInst’), and is even better than many methods with ResNet-101 backbone. We can observe that the main improvement comes from the medium (AP_M) and large (AP_L) objects.

5 Discussion

Limitations. We also observe a few limitations of our method. First, the performance of the model may be limited by the representation of the language model. Zero-shot categories with very similar semantic expressions may be confused. Second, the model may fail to generalize to classes that are too far from the training language space. However, we believe that if merging data with more categories in our method, we can

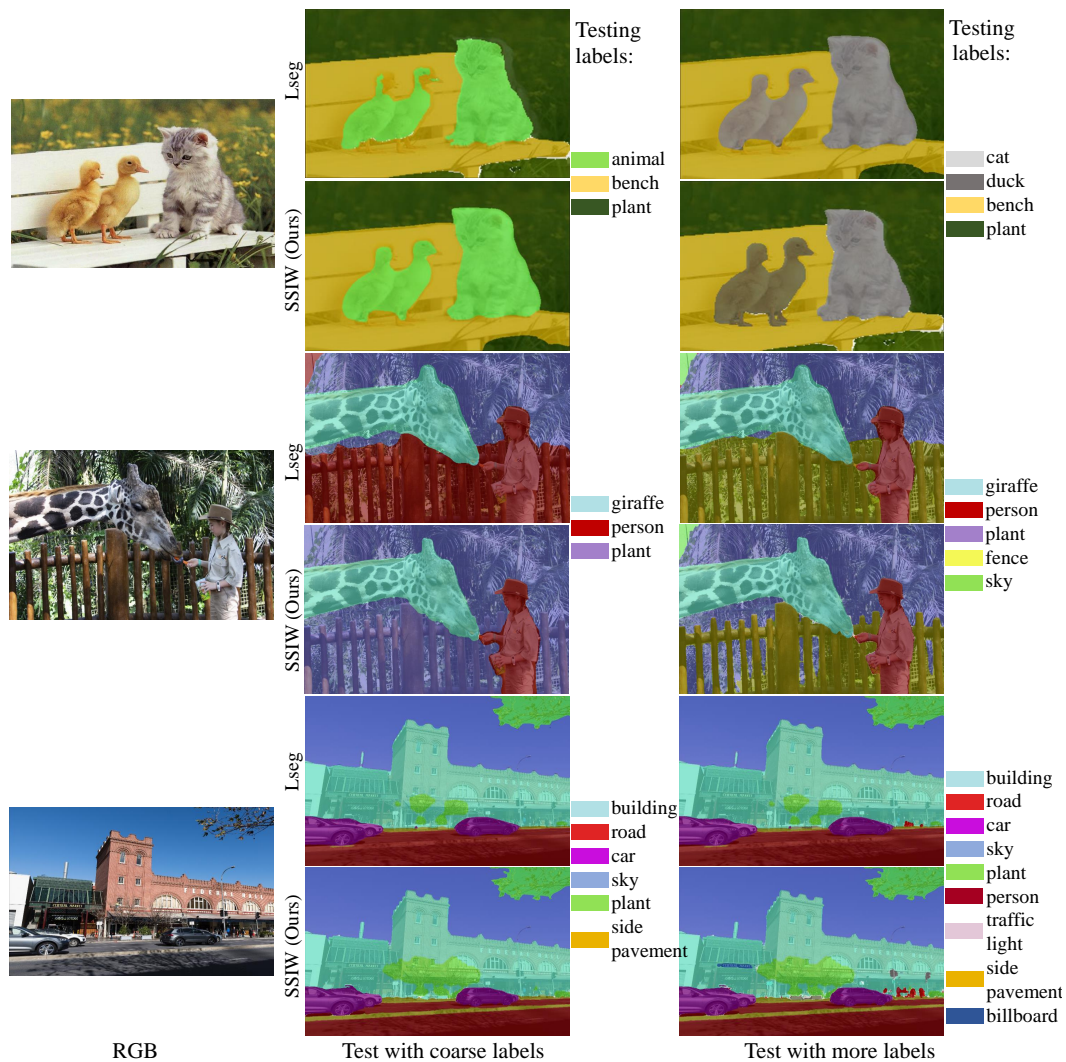


Fig. 8 Comparison with Lseg [13] on web images. We collect several online photos and test them with different label sets. We test on two different label sets, i.e. one has coarse labels, while the other one has more refined labels. Our method can segment better on the refined label set.

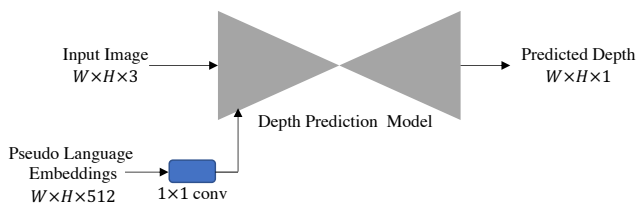


Fig. 9 **Depth Prediction Framework.** The language embeddings are input to the depth prediction network.

achieve more distinguishable features and alleviate this problem. The improvement of the language model may also benefit the proposed method.

Conclusion. In this work, we have proposed an approach to semantic segmentation that can achieve promising performance over multiple zero-shot cross-domain datasets. By collecting short label descriptions from Wikipedia and encoding them in vector-valued embed-

dings to replace labels, we can easily merge multiple datasets together to retrieve a strong and robust segmentation model. A heterogeneous loss is proposed to leverage noisy datasets and weakly annotated datasets. Extensive experiments demonstrate that we can achieve better or comparable performance with current state-of-the-art methods on 7 cross-domain datasets. Furthermore, our resulting model demonstrates the ability to segment some zero-shot labels. With our robust and strong model, the downstream applications can also be boosted significantly.

Acknowledgements Part of this work was done when Wei Yin was an intern at Amazon.

NYUDV2		Pascal Context	
mIoU (ss)			
MTI-Net [56]	49.0	OCR [57]	59.6
ICM [58]	50.7	CAA [59]	60.5
ShapeConv [60]	51.3	DPT [61]	60.5
HRNet (ImageNet)	44.5	HRNet [52]	50.3
HRNet (Mseg)	53.4	HRNet (Mseg)	52.6
HRNet (Ours)	54.1	HRNet (Ours)	52.8
Segformer (ImageNet)	50.0	Segformer (ImageNet)	59.4
Segformer (ADE20K)	59.1	Segformer (ADE20K)	60.8
Segformer (Ours)	60.0	Segformer (Ours)	65.0

Table 8 Fine tuning on small datasets. Our well-trained weight can provide strong performance on NYU and Pascal Context, which surpasses the state-of-the-art methods by a large margin.

Method	Backbone	NYU		KITTI		DIODE		ScanNet		Sintel	
		AbsRel↓	δ_1 ↑	AbsRel↓	δ_1 ↑	AbsRel↓	δ_1 ↑	AbsRel↓	δ_1 ↑	AbsRel↓	δ_1 ↑
OASIS [62]	ResNet50	21.9	66.8	31.7	43.7	48.4	53.4	19.8	69.7	60.2	42.9
MegaDepth [63]	Hourglass	19.4	71.4	20.1	66.3	39.1	61.5	19.0	71.2	39.8	52.7
Xian <i>et al.</i> [64]	ResNet50	16.6	77.2	27.0	52.9	42.5	61.8	17.4	75.9	52.6	50.9
DiverseDepth [28] [53]	ResNeXt50	11.7	87.5	19.0	70.4	37.6	63.1	10.8	88.2	38.6	58.7
MiDaS [31]	ResNeXt101	11.1	88.5	23.6	63.0	33.2	71.5	11.1	88.6	40.5	60.6
LeReS [32]	ResNet50	9.1	91.4	14.3	80.0	28.7	75.1	9.6	90.8	34.4	62.4
Ours + LeReS	ResNet50	8.6	92.3	14.0	80.6	27.4	75.8	8.0	93.4	29.2	62.4

Table 9 Quantitative comparison of our depth prediction with state-of-the-art methods on five zero-shot (unseen during training) datasets. Our method input with pseudo semantic labels achieves much better performance than existing state-of-the-art methods across all test datasets.

Method	Backbone	Schedule	AP (%)	AP ₅₀	AP ₇₅	AP _S	AP _M	AP _L
Mask R-CNN [65]	R-50-FPN	3×	37.5	59.3	40.2	21.1	39.6	48.3
TensorMask [66]	R-50-FPN	6×	35.4	57.2	37.3	16.3	36.8	49.3
BlendMask [67]	R-50-FPN	3×	37.0	58.9	39.7	17.3	39.4	52.5
CondInst (10%COCO*)	R-50-FPN	1×	21.7	35.2	22.0	8.9	22.4	31.1
Ours (CondInst), 10%COCO*	R-50-FPN	1×	33.2	52.1	35.2	15.0	36.4	48.0
CondInst (25%COCO*)	R-50-FPN	1×	31.4	50.6	33.1	14.5	34.2	45.9
Ours (CondInst), 25%COCO*	R-50-FPN	1×	36.4	56.9	38.6	17.7	39.4	53.0
CondInst [68]	R-50-FPN	1×	35.9	57.0	38.2	19.0	40.3	48.7
Ours (CondInst), 50%COCO*	R-50-FPN	1×	38.1	59.0	40.8	18.7	41.5	55.2
Ours (CondInst), COCO	R-50-FPN	1×	39.5	60.7	42.5	19.5	42.9	57.5
Mask R-CNN	R-101-FPN	6×	38.3	61.2	40.8	18.2	40.6	54.1
PolarMask [69]	R-101-FPN	2×	32.1	53.7	33.1	14.7	33.8	45.3
TensorMask	R-101-FPN	6×	37.1	59.3	39.4	17.4	39.1	51.6
BlendMask	R-101-FPN	3×	39.6	61.6	42.6	22.4	42.2	51.4
SOLOv2 [70]	R-101-FPN	6×	39.7	60.7	42.9	17.3	42.9	57.4
CondInst	R-101-FPN	3×	40.0	62.0	42.9	21.4	42.6	53.0
CondInst	R-101-BiFPN	3×	40.5	62.4	43.4	21.8	43.3	53.3
Ours (CondInst)	R-101-BiFPN	3×	41.4	63.0	44.7	20.0	45.5	59.5

Table 10 Quantitative comparison of our instance segmentation with state-of-the-art methods on COCO. With our created pseudo labels on Objects365, the performance is improved significantly. * Used 10% ~ 50% of COCO data for training.

References

1. N. Silberman, D. Hoiem, P. Kohli, and R. Fergus, “Indoor segmentation and support inference from rgb-d images,” in *Eur. Conf. Comput. Vis.* Springer, 2012, pp. 746–760.
2. M. Everingham, S. A. Eslami, L. Van Gool, C. K. Williams, J. Winn, and A. Zisserman, “The pascal visual object classes challenge: A retrospective,” *Int. J. Comput. Vis.*, vol. 111, no. 1, pp. 98–136, 2015.
3. M. Cordts, M. Omran, S. Ramos, T. Rehfeld, M. Enzweiler, R. Benenson, U. Franke, S. Roth, and B. Schiele, “The cityscapes dataset for semantic urban scene understanding,” in *IEEE Conf. Comput. Vis. Pattern Recog.*, 2016, pp. 3213–3223.
4. T.-Y. Lin, M. Maire, S. Belongie, J. Hays, P. Perona, D. Ramanan, P. Dollár, and C. L. Zitnick, “Microsoft coco: Common objects in context,” in *Eur. Conf. Comput. Vis.* Springer, 2014, pp. 740–755.
5. Y. Xian, S. Choudhury, Y. He, B. Schiele, and Z. Akata, “Semantic projection network for zero-and few-label semantic segmentation,” in *IEEE Conf. Comput. Vis. Pattern Recog.*, 2019, pp. 8256–8265.

6. P. Hu, S. Sclaroff, and K. Saenko, "Uncertainty-aware learning for zero-shot semantic segmentation." *Adv. Neural Inform. Process. Syst.*, vol. 3, p. 5, 2020.
7. D. Baek, Y. Oh, and B. Ham, "Exploiting a joint embedding space for generalized zero-shot semantic segmentation," in *Int. Conf. Comput. Vis.*, 2021, pp. 9536–9545.
8. H. Zhao, X. Puig, B. Zhou, S. Fidler, and A. Torralba, "Open vocabulary scene parsing," in *Int. Conf. Comput. Vis.*, 2017, pp. 2002–2010.
9. J. Lambert, Z. Liu, O. Sener, J. Hays, and V. Koltun, "MSeg: A composite dataset for multi-domain semantic segmentation," in *IEEE Conf. Comput. Vis. Pattern Recog.*, 2020.
10. A. Radford, J. W. Kim, C. Hallacy, A. Ramesh, G. Goh, S. Agarwal, G. Sastry, A. Askell, P. Mishkin, J. Clark *et al.*, "Learning transferable visual models from natural language supervision," *arXiv: Comp. Res. Repository*, p. 2103.00020, 2021.
11. R. Benenson, S. Popov, and V. Ferrari, "Large-scale interactive object segmentation with human annotators," in *IEEE Conf. Comput. Vis. Pattern Recog.*, 2019.
12. S. Shao, Z. Li, T. Zhang, C. Peng, G. Yu, X. Zhang, J. Li, and J. Sun, "Objects365: A large-scale, high-quality dataset for object detection," in *Int. Conf. Comput. Vis.*, 2019, pp. 8430–8439.
13. B. Li, K. Q. Weinberger, S. Belongie, V. Koltun, and R. Ranftl, "Language-driven semantic segmentation," in *Int. Conf. Learn. Represent.*, 2022.
14. J. Long, E. Shelhamer, and T. Darrell, "Fully convolutional networks for semantic segmentation," in *IEEE Conf. Comput. Vis. Pattern Recog.*, 2015, pp. 3431–3440.
15. E. Xie, W. Wang, Z. Yu, A. Anandkumar, J. M. Alvarez, and P. Luo, "SegFormer: Simple and efficient design for semantic segmentation with transformers," *Adv. Neural Inform. Process. Syst.*, 2021.
16. Z. Liu, Y. Lin, Y. Cao, H. Hu, Y. Wei, Z. Zhang, S. Lin, and B. Guo, "Swin transformer: Hierarchical vision transformer using shifted windows," *Int. Conf. Comput. Vis.*, 2021.
17. O. Zendel, K. Honauer, M. Murschitz, D. Steininger, and G. F. Dominguez, "Wilddash-creating hazard-aware benchmarks," in *Eur. Conf. Comput. Vis.* Springer, 2018, pp. 402–416.
18. B. Cheng, A. G. Schwing, and A. Kirillov, "Per-pixel classification is not all you need for semantic segmentation," 2021.
19. B. Cheng, I. Misra, A. G. Schwing, A. Kirillov, and R. Girdhar, "Masked-attention mask transformer for universal image segmentation," 2022.
20. M. Bucher, T.-H. Vu, M. Cord, and P. Pérez, "Zero-shot semantic segmentation," *Adv. Neural Inform. Process. Syst.*, vol. 32, pp. 468–479, 2019.
21. Z. Gu, S. Zhou, L. Niu, Z. Zhao, and L. Zhang, "Context-aware feature generation for zero-shot semantic segmentation," in *ACM Int. Conf. Multimedia*, 2020, pp. 1921–1929.
22. J. Ding, N. Xue, G.-S. Xia, and D. Dai, "Decoupling zero-shot semantic segmentation," 2022.
23. G. A. Miller, "Wordnet: a lexical database for english," *Communications of the ACM*, vol. 38, no. 11, pp. 39–41, 1995.
24. G. Ros, S. Stent, P. F. Alcantarilla, and T. Watanabe, "Training constrained deconvolutional networks for road scene semantic segmentation," *arXiv: Comp. Res. Repository*, p. 1604.01545, 2016.
25. P. Bevandić, I. Krešo, M. Oršić, and S. Šegvić, "Simultaneous semantic segmentation and outlier detection in presence of domain shift," in *German Conf. Pattern Recog.* Springer, 2019, pp. 33–47.
26. K. Xian, C. Shen, Z. Cao, H. Lu, Y. Xiao, R. Li, and Z. Luo, "Monocular relative depth perception with web stereo data supervision," in *IEEE Conf. Comput. Vis. Pattern Recog.*, 2018, pp. 311–320.
27. W. Chen, Z. Fu, D. Yang, and J. Deng, "Single-image depth perception in the wild," in *Adv. Neural Inform. Process. Syst.*, 2016, pp. 730–738.
28. W. Yin, X. Wang, C. Shen, Y. Liu, Z. Tian, S. Xu, C. Sun, and D. Renyin, "Diversedepth: Affine-invariant depth prediction using diverse data," *arXiv: Comp. Res. Repository*, p. 2002.00569, 2020.
29. W. Yin, C. Zhang, H. Chen, Z. Cai, G. Yu, K. Wang, X. Chen, and C. Shen, "Metric3d: Towards zero-shot metric 3d prediction from a single image," *Int. Conf. Comput. Vis.*, 2023.
30. W. Yin, J. Zhang, O. Wang, S. Niklaus, S. Chen, Y. Liu, and C. Shen, "Towards accurate reconstruction of 3d scene shape from a single monocular image," *IEEE Trans. Pattern Anal. Mach. Intell.*, 2022.
31. R. Ranftl, K. Lasinger, D. Hafner, K. Schindler, and V. Koltun, "Towards robust monocular depth estimation: Mixing datasets for zero-shot cross-dataset transfer," *IEEE Trans. Pattern Anal. Mach. Intell.*, 2020.
32. W. Yin, J. Zhang, O. Wang, S. Niklaus, L. Mai, S. Chen, and C. Shen, "Learning to recover 3d scene shape from a single image," in *IEEE Conf. Comput. Vis. Pattern Recog.*, 2021.
33. T. Mikolov, I. Sutskever, K. Chen, G. S. Corrado, and J. Dean, "Distributed representations of words and phrases and their compositionality," in *Adv. Neural Inform. Process. Syst.*, 2013, pp. 3111–3119.
34. S. Bujwid and J. Sullivan, "Large-scale zero-shot image classification from rich and diverse textual descriptions," *arXiv: Comp. Res. Repository*, 2021.
35. B. Zhou, H. Zhao, X. Puig, S. Fidler, A. Barriuso, and A. Torralba, "Scene parsing through ade20k dataset," in *IEEE Conf. Comput. Vis. Pattern Recog.*, 2017.
36. G. Neuhold, T. Ollmann, S. Rota Bulò, and P. Kotschieder, "The mapillary vistas dataset for semantic understanding of street scenes," in *Int. Conf. Comput. Vis.*, 2017, pp. 4990–4999.
37. G. Varma, A. Subramanian, A. Namboodiri, M. Chandraker, and C. Jawahar, "Idd: A dataset for exploring problems of autonomous navigation in unconstrained environments," in *IEEE Winter Conf. on Applic. of Comp. Vis.* IEEE, 2019, pp. 1743–1751.
38. F. Yu, H. Chen, X. Wang, W. Xian, Y. Chen, F. Liu, V. Madhavan, and T. Darrell, "Bdd100k: A diverse driving dataset for heterogeneous multitask learning," in *IEEE Conf. Comput. Vis. Pattern Recog.*, June 2020.
39. S. Song, S. P. Lichtenberg, and J. Xiao, "Sun rgb-d: A rgb-d scene understanding benchmark suite," in *IEEE Conf. Comput. Vis. Pattern Recog.*, 2015, pp. 567–576.
40. G. Brostow, J. Shotton, J. Fauqueur, and R. Cipolla, "Segmentation and recognition using structure from motion point clouds," in *Eur. Conf. Comput. Vis.* Springer, 2008, pp. 44–57.
41. R. Mottaghi, X. Chen, X. Liu, N.-G. Cho, S.-W. Lee, S. Fidler, R. Urtasun, and A. Yuille, "The role of context for object detection and semantic segmentation in the wild," in *IEEE Conf. Comput. Vis. Pattern Recog.*, 2014, pp. 891–898.
42. A. Geiger, P. Lenz, C. Stiller, and R. Urtasun, "Vision meets robotics: The kitti dataset," *Int. J. of Rob. Research*, 2013.

43. I. Vasiljevic, N. Kolkin, S. Zhang, R. Luo, H. Wang, F. Z. Dai, A. F. Daniele, M. Mostajabi, S. Basart, M. R. Walter, and G. Shakhnarovich, "DIODE: A Dense Indoor and Outdoor DEpth Dataset," *arXiv: Comp. Res. Repository*, vol. 1908.00463, 2019. [Online]. Available: <http://arxiv.org/abs/1908.00463>
44. A. Dai, A. X. Chang, M. Savva, M. Halber, T. Funkhouser, and M. Nießner, "Scannet: Richly-annotated 3d reconstructions of indoor scenes," in *IEEE Conf. Comput. Vis. Pattern Recog.*, 2017, pp. 5828–5839.
45. D. J. Butler, J. Wulff, G. B. Stanley, and M. J. Black, "A naturalistic open source movie for optical flow evaluation," in *Eur. Conf. Comput. Vis.*, 2012, pp. 611–625.
46. L. Yang, Y. Fan, and N. Xu, "Video instance segmentation," in *Int. Conf. Comput. Vis.*, 2019, pp. 5188–5197.
47. Y. Zhu, K. Sapra, F. A. Reda, K. J. Shih, S. Newsam, A. Tao, and B. Catanzaro, "Improving semantic segmentation via video propagation and label relaxation," in *IEEE Conf. Comput. Vis. Pattern Recog.*, 2019, pp. 8856–8865.
48. Ö. Erkent and C. Laugier, "Semantic segmentation with unsupervised domain adaptation under varying weather conditions for autonomous vehicles," *IEEE Robotics and Automation Letters*, vol. 5, no. 2, pp. 3580–3587, 2020.
49. C. Liu, L.-C. Chen, F. Schroff, H. Adam, W. Hua, A. L. Yuille, and L. Fei-Fei, "Auto-deeplab: Hierarchical neural architecture search for semantic image segmentation," in *IEEE Conf. Comput. Vis. Pattern Recog.*, 2019, pp. 82–92.
50. L.-C. Chen, Y. Zhu, G. Papandreou, F. Schroff, and H. Adam, "Encoder-decoder with atrous separable convolution for semantic image segmentation," in *Eur. Conf. Comput. Vis.* Springer, 2018, pp. 801–818.
51. A. Valada, R. Mohan, and W. Burgard, "Self-supervised model adaptation for multimodal semantic segmentation," *Int. J. Comput. Vis.*, vol. 128, no. 5, pp. 1239–1285, 2020.
52. K. Sun, B. Xiao, D. Liu, and J. Wang, "Deep high-resolution representation learning for human pose estimation," in *IEEE Conf. Comput. Vis. Pattern Recog.*, 2019.
53. W. Yin, Y. Liu, and C. Shen, "Virtual normal: Enforcing geometric constraints for accurate and robust depth prediction," *IEEE Transactions on Pattern Analysis and Machine Intelligence (TPAMI)*, 2021.
54. L. Porzi, S. Rota Bulò, A. Colovic, and P. Kotschieder, "Seamless scene segmentation," in *IEEE Conf. Comput. Vis. Pattern Recog.*, June 2019.
55. L. Yang, Y. Fan, and N. Xu, "Video instance segmentation," *arXiv: Comp. Res. Repository*, vol. 1905.04804, 2019. [Online]. Available: <https://arxiv.org/abs/1905.04804>
56. S. Vandenhende, S. Georgoulis, and L. Van Gool, "Mtinnet: Multi-scale task interaction networks for multi-task learning," in *Eur. Conf. Comput. Vis.* Springer, 2020, pp. 527–543.
57. Y. Yuan, X. Chen, and J. Wang, "Object-contextual representations for semantic segmentation," in *Eur. Conf. Comput. Vis.* Springer, 2020, pp. 173–190.
58. H. Shi, H. Li, Q. Wu, and Z. Song, "Scene parsing via integrated classification model and variance-based regularization," in *IEEE Conf. Comput. Vis. Pattern Recog.*, 2019, pp. 5307–5316.
59. Y. Huang, W. Jia, X. He, L. Liu, Y. Li, and D. Tao, "Channelized axial attention for semantic segmentation," *arXiv: Comp. Res. Repository*, p. 2101.07434, 2021.
60. J. Cao, H. Leng, D. Lischinski, D. Cohen-Or, C. Tu, and Y. Li, "Shapeconv: Shape-aware convolutional layer for indoor rgb-d semantic segmentation," *arXiv: Comp. Res. Repository*, p. 2108.10528, 2021.
61. R. Ranftl, A. Bochkovskiy, and V. Koltun, "Vision transformers for dense prediction," in *Int. Conf. Comput. Vis.*, 2021, pp. 12 179–12 188.
62. W. Chen, S. Qian, D. Fan, N. Kojima, M. Hamilton, and J. Deng, "Oasis: A large-scale dataset for single image 3d in the wild," in *IEEE Conf. Comput. Vis. Pattern Recog.*, 2020, pp. 679–688.
63. Z. Li and N. Snavely, "Megadepth: Learning single-view depth prediction from internet photos," in *IEEE Conf. Comput. Vis. Pattern Recog.*, 2018, pp. 2041–2050.
64. K. Xian, J. Zhang, O. Wang, L. Mai, Z. Lin, and Z. Cao, "Structure-guided ranking loss for single image depth prediction," in *IEEE Conf. Comput. Vis. Pattern Recog.*, 2020, pp. 611–620.
65. K. He, G. Gkioxari, P. Dollár, and R. Girshick, "Mask r-cnn," in *Int. Conf. Comput. Vis.*, 2017, pp. 2961–2969.
66. X. Chen, R. Girshick, K. He, and P. Dollár, "TensorMask: A foundation for dense object segmentation," in *Int. Conf. Comput. Vis.*, 2019, pp. 2061–2069.
67. H. Chen, K. Sun, Z. Tian, C. Shen, Y. Huang, and Y. Yan, "BlendMask: Top-down meets bottom-up for instance segmentation," in *IEEE Conf. Comput. Vis. Pattern Recog.*, 2020.
68. Z. Tian, C. Shen, and H. Chen, "Conditional convolutions for instance segmentation," in *Eur. Conf. Comput. Vis.* Springer, 2020.
69. E. Xie, P. Sun, X. Song, W. Wang, X. Liu, D. Liang, C. Shen, and P. Luo, "Polarmask: Single shot instance segmentation with polar representation," in *IEEE Conf. Comput. Vis. Pattern Recog.*, 2020, pp. 12 193–12 202.
70. X. Wang, R. Zhang, T. Kong, L. Li, and C. Shen, "SOLOv2: Dynamic and fast instance segmentation," in *Adv. Neural Inform. Process. Syst.*, 2020.
71. A. Zamir, A. Sax, W. Shen, L. Guibas, J. Malik, and S. Savarese, "Taskonomy: Disentangling task transfer learning," in *IEEE Conf. Comput. Vis. Pattern Recog.* IEEE, 2018.
72. Y. Kim, H. Jung, D. Min, and K. Sohn, "Deep monocular depth estimation via integration of global and local predictions," *IEEE Trans. Image Process.*, vol. 27, no. 8, pp. 4131–4144, 2018.
73. Y. Hua, P. Kohli, P. Uplavikar, A. Ravi, S. Gunaseelan, J. Orozco, and E. Li, "Holopix50k: A large-scale in-the-wild stereo image dataset," in *IEEE Conf. Comput. Vis. Pattern Recog. Worksh.*, June 2020.